TECHNICAL REPORT NO. 8

BUBBLE GROWTH RATES IN BOILING

BY PETER GRIFFITH

THE OFFICE OF NAVAL RESEARCH
CONTRACT N5ori-07827
NR-035-267
D.I.C. PROJECT NUMBER 5-7348

AND

THE NATIONAL SCIENCE FOUNDATION
GRANT NUMBER NSFG1706
D.I.C. PROJECT NUMBER 5-7374

JUNE 1956

GRANT NUMBER NSFG-1706

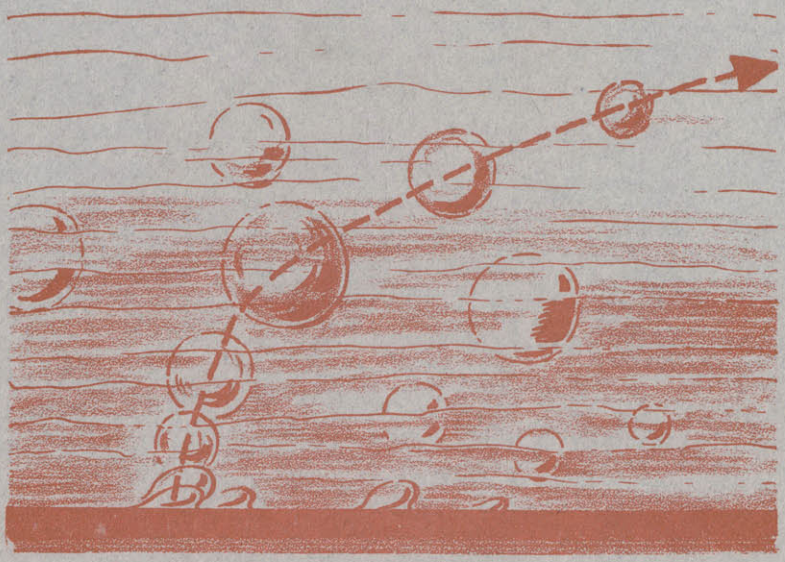

MASSACHUSETTS INSTITUTE OF TECHNOLOGY
DIVISION OF INDUSTRIAL COOPERATION
CAMBRIDGE 39, MASSACHUSETTS

BUBBLE GROWTH RATES IN BOILING

By

Peter Griffith *

ABSTRACT

The conditions determining the growth rate of a bubble on a surface in boiling are considered and a mathematical model framed in the light of these conditions. The growth rate is then calculated for bubbles growing under a range of conditions of pressure, wall superheat and bulk fluid temperature. The average growth rate of a bubble is found to decrease with increasing maximum size and to decrease with increasing pressure. At high pressure the maximum size of the bubble is found to be independent of pressure and primarily a function of the thickness of the superheated layer near the surface. The calculated bubble growth velocities are then used to correlate some burnout data for a variety of fluids under a range of pressures in pool boiling. Bubble growth pictures are presented for water at atmospheric pressure under a variety of conditions.

---

* Assistant Professor of Mechanical Engineering, Massachusetts Institute of Technology, Cambridge, Massachusetts.

INTRODUCTION

Studies of the mechanism of nucleate boiling indicate the principal mode of heat transfer is from the surface to the liquid with the bubbles acting as turbulence promoters (6, 3). Correlations for predicting both the heat flux-temperature difference relation and the maximum heat flux attainable in nucleate boiling depend in part on the characteristic growth velocity for the bubbles. Ellion (3) used a measured growth velocity for correlation. Forester and Zuber (1, 2) calculated a growth velocity assuming the bubbles were growing in an initially uniformly superheated liquid. Under these conditions the bubbles continue to grow without limit, while with subcooled liquid the bubbles grow only to a maximum size. Rohsenow (8) and Rohsenow and Griffith (7) assumed that the growth velocity was not an important variable in the correlation. Further advances in the correlation of boiling heat transfer data and a better understanding of the boiling heat transfer process depend on obtaining the growth curves for bubbles growing under nucleate boiling conditions. In particular, it is desirable to know the effect of the system pressure and subcooling in the bulk of the liquid on the maximum bubble size attained and the time it takes to attain this size.

I THE BUBBLE GROWTH PROBLEM

Though the earliest stages of a bubble's life are important for a complete understanding of bubble formation and growth (4, 2), the principal stirring in the liquid is accomplished during the later, or asymptotic stages, of bubble growth. This stage includes virtually the entire visible life of bubbles at moderate and high pressures and most of the life of a bubble at low pressures.

The asymptotic stage of growth is characterized by negligible surface tension and dynamic effects so that the growth rate of the bubble is dependent essentially on the heat transfer in the liquid to the bubble wall. It is therefore appropriate to begin by examining the conditions existing in the liquid when the bubble starts to grow; then, on the basis of these conditions, postulate a mathematical model and finally solve for the bubble radius time curve.

Bubble growth occurs as a result of evaporation at the bubble wall. The heat for this evaporation is transferred by conduction from the surrounding liquid. If a laminar flow field and constant properties are assumed in the liquid surrounding the bubble, the equation governing the heat transfer process is,

$$\nabla^2 T = \frac{\rho_\ell c_\ell}{k_\ell}\left[\frac{\partial T}{\partial t} + \bar{V} \cdot \nabla T\right] \tag{1}$$

If the bubble is assumed to consist of a spherical segment, the heat transfer at the bubble wall is

$$q = -k_\ell \int_A \left(\frac{\partial T}{\partial r}\right)_{r=R} dA \tag{2}$$

The rate of evaporation can be related to the rate of growth of the bubble through the First Law of Thermodynamics. Consider the system illustrated in Figure 1. At time one it consists of a small mass of superheated liquid, and at time two it consists of the same mass evaporated into vapor. The shape has been taken as hemispherical as a bubble in its early stages closely approximates this shape. This is shown in Figure 10 and explained in greater detail in Section III. In addition the fluid flow pattern around a hemispherical bubble on a surface is simple and easy to handle analytically. If it is assumed the latent heat of vaporization is large compared to any superheat enthalpy in the original liquid and that the growth occurs essentially at constant pressure, the First Law of Thermodynamics yields

$$Q = wh_{fg} \tag{3}$$

When the mass within the bubble is expressed in terms of the density and volume and (3) is differentiated with respect to time

$$q = 2\pi R^2 \rho_v h_{fg}\left(\frac{dR}{dt}\right) \tag{4}$$

Eliminate q between Equations (2) and (4) and express the area in spherical coordinates then

$$\frac{dR}{dt} = -\frac{k_\ell}{\rho_v h_{fg}} \int_0^{\frac{\pi}{2}} \left(\frac{\partial T}{\partial r}\right)_{r=R} \sin\varphi \, d\varphi \tag{5}$$

Continuity considerations relate the velocity at any point to the velocity of the bubble wall which is expressed in Equation (5).

$$V = -\frac{R^2}{r^2}\left(\frac{k_\ell}{\rho_v h_{fg}}\right) \int_0^{\frac{\pi}{2}} \left(\frac{\partial T}{\partial r}\right)_{r=R} \sin\varphi \, d\varphi \tag{6}$$

Together with the appropriate initial and boundary conditions, Equations (1) and (6) specify the bubble growth problem.

INITIAL AND BOUNDARY CONDITIONS

As essentially all of the visible life of a bubble occurs during the asymptotic stage of growth in which the surface tension and dynamic effects are negligible, the pressure within the bubble is essentially the same as that existing well outside the bubble. Therefore, the bubble wall temperature is very close to saturation temperature for that pressure.

$$T = T_s \text{ at } R = r \tag{7}$$

The heater surface temperature has been taken as constant.

$$T = T_w \text{ at } \varphi = \pi/2 \tag{8}$$

Actually, as the bubbles grow and depart, the surface varies in temperature, but whether these fluctuations are significant compared to those experienced by the liquid determines whether the surface can be considered at constant temperature. A rough idea of the relative magnitude of these fluctuations can be obtained by imagining a very simple ideal case. Consider a semi-infinite slab of heater material at a high temperature brought in contact with another semi-infinite slab of liquid at saturation temperature. What will be the temperature assumed by the interface? For the combination water and copper, temperature of the water at the interface increases 23 times as much as that of the copper decreases. For water and stainless steel the water, temperature increases 5 times as much. These two surfaces represent the extremes in surface properties so the assumption of constant surface temperature is probably quite good. The points common to both the bubble and surface have been taken at saturation temperature because if their temperature were significantly above it, there would be a very large evaporation rate at that point which would soon cool it down to close to saturation temperature.

The initial conditions are fixed by considering the bubble's environment at the instant it starts to grow. In general there is a thin layer of superheated liquid in the vicinity of the wall whether there is pool boiling or boiling in the presence of forced convection. The thickness of this layer would be determined by the forced or natural convection in the fluid and the unsteady heat transfer to the liquid rushing in when a bubble departs or collapses. Figure 2 illustrates the likely temperature distribution along with the one assumed in these calculations. Though this is not the best possible assumption, it is simple and is characterized by one parameter "b" the distance from the wall to the point where the temperature

is constant at T_b. An initial radius is also assumed in order to start the solution. These initial conditions are

$$T = (T_w - T_b)(1 - r\cos\varphi) + T_w \text{ for } r\cos\varphi < b \tag{9}$$

$$T = T_b \text{ for } r\cos\varphi \geqslant 1 \tag{10}$$

$$r = R_o \tag{11}$$

a radius less than the thickness of the superheated layer near the surface and small enough so that the radius assumed will not materially affect the result.

THE SOLUTION

In order to facilitate the solution of this problem it is convenient to transform it into dimensionless form.* For this the length "b" is used as the only significant length in the problem along with the fluid properties as they are all invariant. These dimensionless quantities are defined in the list of symbols. When Equation (6) is expressed in dimensionless form one gets

$$v = -\left(\frac{r^3}{y^2}\right)\frac{\rho_\ell c_\ell (T_w - T_b)}{\rho_v h_{fg}}\int_0^{\frac{\pi}{2}}\left(\frac{\partial\theta}{\partial y}\right)_{y=Y}\sin\varphi\, d\varphi \tag{12}$$

Equation (1) expanded in dimensionless form becomes

$$\frac{1}{y^2}\frac{\partial}{\partial y}\left[y^2\frac{\partial\theta}{\partial y}\right] + \frac{1}{y^2\sin\varphi}\frac{\partial}{\partial\varphi}\left[\sin\varphi\left(\frac{\partial\theta}{\partial\varphi}\right)\right] = \frac{\partial\theta}{\partial\tau} + v\frac{\partial\theta}{\partial y} \tag{13}$$

The initial conditions become

$\theta = (1 - y\cos\varphi)$ for $y\cos\varphi < 1$

$\theta = 0$ for $y\cos\varphi \geqslant 1$

$\theta = \theta_s$ for $y = r$

$Y = Y_o$ a small number

and the boundary conditions

$\theta = \theta_s$ for $y = r$

$\theta = 1$ for $y = 0$.

There are two parameters of significance; a temperature parameter measuring the degree of subcooling, $T_w - T_s/T_w - T_b$ and a properties parameter which is the ratio of the superheat enthalpy per unit volume to the latent heat enthalpy per

---

* Dimensionless symbols defined in Appendix C.

unit volume of the vapor

$$c_1 = \frac{\rho_\ell \, c_\ell (T_w - T_s)}{\rho_v h_{fg}}$$

Equations (12) and (13) have been put into finite difference form and placed on Whirlwind computer for a variety of the parameters.

RESULTS

The computer results are presented in Figures 4 through 8. The range of parameters is sufficient to cover most liquids from 0.1 to 0.9 of the critical pressure at a temperature difference corresponding to the maximum heat flux.

A check on the mathematical solution was obtained by running a program for an initially uniformly isothermal field, then allowing the bubble to grow and comparing the enthalpy defect in the liquid with the enthalpy gain in the bubble. Most of the deviation is due to a first derivative truncation error which decreased as the temperature gradients in the liquid became less. Therefore, the errors would tend to be smaller for the non-isothermal initial conditions as the temperature gradients tend to be less. The approximate deviations are presented in Table 1.

Table 1

$\frac{\rho_\ell \, c_\ell (T_w - T_s)}{\rho_v h_{fg}}$	% error in Y
10.6	12%
5.3	10%
1.0	1%
0.35	1%

A check on the mathematical model is provided by the data of Dergarbedian (5) which is presented in Figure 3. The dots are points measured from high speed motion pictures and the curve is obtained by interpolation of computer results presented in Figure 8. The interpolation is simple as these curves are parabolas.

The range covered by the computer results was limited by the validity of the mathematical model. For very large values of the parameter "c_1" the assumption that the dynamic effects are unimportant is not valid while for small values of this parameter the time the bubble takes to grow and the thickness of the cooled layer surrounding the bubble are so large, the assumed laminar flow field is

probably seriously in error. It was for this last reason also that the course of the bubble was not traced into the collapse region.

The results are in the form of plots of dimensionless radius versus dimensionless time with dimensionless velocity as a parameter. There are three sets of these curves for different values of "c_1", the reciprocal of which is roughly proportional to the thickness of the cooled layer surrounding the bubble. For each value of "c_1", there are three radius-time curves for different values of the bulk temperature and the ends of all these curves are connected by the zero velocity line. The radius of the bubble intersecting the zero velocity line is the maximum radius attained by that bubble. When there is no subcooling in the liquid the bubble radius continues to grow without limit so there is no intersection with the zero velocity line.

Several interesting conclusions can be drawn from these calculations alone. The temperature distributions obtained from the computer made it apparent that for small values of "c_1" the thickness of the cooled layer of liquid surrounding the bubble is large compared to the radius of the bubble. This means that for small "c_1" the plane approximation, used to solve the heat transfer problem by other investigators (2, 4), is inadequate here. For $c_1 = 5$, the plane approximation error is 10%. For "c_1" less than this, the error would increase. It was also apparent from these temperature distributions that for $c_1 = 0.35$ a significant quantity of heat was transferred from the surface to the liquid and then to the bubble wall while the bubble was growing. At higher values of "c_1" corresponding to low pressure this does not happen. Under these conditions the bubble grows primarily as a result of heat transfer from liquid superheated before the bubble ever started to grow.

The calculated growth curves showed that for small "c_1" the maximum size attained by the bubble is proportional to the thickness of the layer of superheated liquid near the surface and is independent of "c_1". In part, this would account for the relatively constant maximum bubble size which has been observed over a wide range of pressure at elevated pressure. Finally, it is apparent from the shape of the line where $v = 0$ on Figures 4, 5, and 6, that even at a constant value of "c_1" the average velocity of growth for a bubble which is equal to I/τ at $v = 0$, decreases with decreasing maximum size. This checks with the experimental observations of Ellion (3).

Though the calculated growth curves are of significance in correlating both q/A vs ΔT data and burnout data, only an application to pool boiling burnout will be presented here. This is because it is necessary to have more information about bubble motions and departures, and about the temperatures existing in the vicinity of the heater than is available at this time.

II POOL BOILING BURNOUT

If an electrically heated wire is immersed in a pool of liquid and the current passing through it is slowly increased, the mode of heat transfer from the wire will pass through several different phases. These various phases are illustrated in Figure 11. The burnout point is the maximum on the curve. If the wire has a low enough melting point, the temperature rise may be severe enough to cause melting of the wire or "burnout". This maximum in the heat flux occurs with all pure liquids no matter what the shape or orientation of the heater surface.

Let us begin by considering the physical conditions at burnout, then, on the basis of these conditions, postulate a burnout criterion and finally check this criterion against burnout data taken under a variety of pressures for different fluids.

As the heat flux in boiling is increased the number of bubbles on the surface also increases. Gunther (9) has a picture taken at 90% burnout heat flux which shows a large glob of vapor at the hot end of a strip with a number of small, discrete bubbles on the rest of the strip. This picture would indicate that when a sufficient number of bubbles are on the surface they are so closely packed, they coalesce and burnout occurs. A criterion for burnout might be that it is necessary for a certain critical packing of bubbles on the surface to exist or, what is equivalent, a critical fraction of wetted surface.

The fraction of wetted surface depends on the conditions in the vicinity of the surface which are quite different for pool boiling, forced convective boiling with subcooled liquid, and forced convective boiling with net generation of vapor. Because of assumptions made in the formulation of the burnout criterion, the result will only apply to regions where there are discrete bubbles present on the surface and further assumptions will limit the application here to pool boiling.

Before beginning, however, one sweeping assumption implicit in the entire analysis should be pointed out. This assumption is that for clean surfaces the surface conditions are not important variables and as such need not be included in the formulation. In leaving the surface conditions out, it is assumed that they are invariable for the data correlated. This assumption is justified, in part, by the fact that all the liquids in contact with clean metal surfaces have 0° contact angles (10). Let us now formulate a burnout criterion. The derivation presented here has also been presented in reference (7).

BURNOUT CORRELATION

Burnout can be visualized as occurring when the packing of bubbles on the

surface reaches some critical fraction of the total area. Figure 12 shows a section of a heater surface with bubbles of constant size packed on it. It is apparent that the number of bubbles per unit area is

$$n = \frac{C_{vb}}{D_b^2} \tag{14}$$

where C_{vb} is a constant which would equal one for the condition illustrated but might be greater or less than unity. We shall assume in any case that at most it varies only with pressure. The heat transferred to the bubbles has been shown (11) to be proportional to the boiling heat transfer so we can write

$$\frac{q}{A}_{\text{boiling}} = C_q h_{fg} \rho_v n (\pi/6) D_b^3 f \tag{15}$$

where C_q is the fraction of heat transferred to the bubbles and f is the frequency that bubbles form at a point. When Eq. (14) is substituted in (15) we get

$$\frac{(q/A)_{max}}{h_{fg} \rho_v (fD_b)} = \frac{\pi}{6} C_q C_{vb} \tag{16}$$

The right side of this expression is a constant or at most a function of pressure. The problem still remains to evaluate (fD_b).

The evaluation of (fD_b) will depend on the system under consideration as the frequency and diameter of the bubbles at the surface have been found to be dependent to some extent on the system pressure and geometry.

EVALUATION OF (fD_b) IN SATURATED POOL BOILING FROM A HORIZONTAL SURFACE

In saturated pool boiling bubbles form on the surface and grow at a decreasing rate until they depart. In order to predict the departure size it is necessary to know the cause of departure. At this time it cannot be said that this is known because departure can be affected by several factors. Perhaps the simplest explanation is that the bubbles depart when the surface forces tending to hold them on the surface are counter balanced by the boyancy forces tending to draw then off. On this assumption Jakob (11) and his co-workers have calculated a criterion for bubble departure which gives the diameter at departure as directly proportional to the contact angle. At high heat fluxes not even approximately static conditions are attained, and furthermore, if this simple static force balance were sufficient to explain departure one would expect a strong dependence of bubble size on heater orientation and contact angle.

An examination of the high speed motion pictures of Figure 10 shows that the bubbles depart essentially perpendicularly from the vertical surface and then rise due to gravity. The most promising explanation suggests that it is due to the inertia of the surrounding liquid. The explanation of how it operates to draw the bubble off the surface is as follows.

In the early stages of growth the velocities are quite high, but as the thickness of the cooled layer of liquid surrounding the bubble becomes greater and as the bubble penetrates into the cooler bulk liquid, its growth rate decreases and the liquid moving away from the surface must be decelerated. In causing this deceleration, the liquid tends to draw the bubble off the surface. The pictures show that when this occurs the bubble growth rate has decreased to a very low value. In the light of this mechanism perhaps a different criterion for departure might be framed. It would be reasonable to have this criterion dependent on the reduction of the growth rate of the bubble to a certain value. Assume then that the bubble will be unable to depart from the surface until its growth rate drops below its rise velocity. This is a necessary condition, but if the contact angle is large enough it may not be the determining one. This model still has the fault that the departure size is sensitive to the strip orientation but the sensitive dependence of the departure bubble size on contact angle is eliminated.

Examination of Figure 10 shows that for the large fraction of the bubble growth period, the bubble has a shape which is well approximated by a hemisphere on the surface. As this is true the calculated radius time curves can be used in calculating the (fD_b) if there were some method of specifying the "b". "b" is the distance assumed for the original straight line temperature gradient. The thickness that should be chosen for this is primarily a function of how long that section of the surface has been free of the vapor. For lack of any better assumption this time has been taken as equal to the life of the bubble on the surface, after Jacob. Actually the pause should be calculable from the properties of the surface and fluid and the temperatures in the surface and fluid after the bubble departs. Now let us collect the observations and assumptions and state them in mathematical form in order to get an expression for (fD_B).

The assumption equating the pause between bubbles to the life of a bubble on the surface allows us to calculate a thermal layer thickness "b". If the liquid next to the surface is treated as an infinite stagnant slab with a step change in temperature put on its surface at the instant the bubble departs, the temperature distribution will follow the error function (11). This is illustrated in Figure 13. The "erf" curve can be approximated by the straight line drawn in and the intersection with the $\theta = 1$ line gives the value of the thermal layer thickness "b".

From the straight line on Figure 13 then

$$b = 2\sqrt{\frac{k_\ell t_b}{\rho_\ell c_\ell}} \tag{17}$$

From the definition of dimensionless time

$$t = \left(\frac{\rho_\ell c_\ell \tau}{k_\ell}\right) b^2 \tag{18}$$

and when "b" is eliminated between Equations (17) and (18) we get

$$\tau = 0.25 \tag{19}$$

The range of bubble sizes encountered in this calculation is such that bubble rise velocity is adequately represented by Stokes Law

$$V_{rise} = \frac{g(\rho_\ell - \rho_v) D_b^2}{18 \mu_\ell} \tag{20}$$

From the definition of the dimensionless growth velocity

$$V_{growth} = \frac{v}{b}\left(\frac{k_\ell}{\rho_\ell c_\ell}\right) \tag{21}$$

The definition of Y gives

$$R = bY \tag{22}$$

The bubble as it grows on the surface is approximately hemispherical, but when it departs, it is approximately spherical. Therefore the diameter of a spherical bubble is wanted which is equivalent in volume to the hemispherical one. This is

$$D_b = 1.59\ bY \tag{23}$$

When Equations (20) and (21) are equated and (23) substituted for D_b, the result can be solved for "b" as follows:

$$b = \left[\frac{18}{(1.59)^2 g}\left(\frac{V}{Y^2}\right)\left(\frac{\mu_\ell}{\rho_\ell - \rho_v}\right)\left(\frac{k_\ell}{\rho_\ell c_\ell}\right)\right]^{1/3} \tag{24}$$

The "v" and the "Y" appearing is this equation are evaluated from Figure 9 at the appropriate value of $\frac{\rho_\ell c_\ell (T_w - T_s)}{\rho_v h_{fg}}$. The (fD_b) then can be calculated without further assumption from

$$(fD_b) = \frac{D_b}{2t_b} \tag{25}$$

When Equations (18), (19), (23), and (24) are substituted in (25) the final expression for (fD_b) is obtained. Thus

$$fD_b = \frac{1.59\ Y}{(2)(0.25)\left[\frac{\rho_l c_l}{k_l}\right]\left[\frac{18}{(1.59)^2 g}\left(\frac{v}{Y^2}\right)\left(\frac{\mu_l}{\rho_l - \rho_v}\right)\left(\frac{k_l}{\rho_l c_l}\right)\right]^{1/3}} \qquad (26)$$

The factor 2 appearing in the denominator of (25) and (26) is a result of the assumption that the pause between bubbles is equal to the bubble life on the surface. If there were no pause, this factor would be unity.

Earlier the constants in Equation (16) were stated to be at most, functions of pressure. The properties of importance which varied primarily with pressure are those in the number "c_1". Why the constant "C_q" in (16) should be a function of "c_1" can be seen most easily be considering the physical significance of "c_1" and then seeing how "C_q" might be affected by it. The numerator of "c_1" is the superheat enthalpy of the liquid per unit volume, and the denominator the latent heat of the vapor per unit volume. When "c_1" is large, a little superheated liquid will form a large volume of vapor, and when it is small only a small volume will be formed. Therefore, the layer of cooled liquid surrounding the bubble is much thicker for small c_1. This is illustrated in Figure 14.

For bubbles of the same size, the area significantly affected by the motion of the bubble will be about the same. Because of the different thermal layer thickness for the two bubbles, however, it is apparent that the fraction of the heat transferred to the bubble will be quite different in comparison to the total heat transfer. Therefore the "C_q" will be different. This suggests plotting the burnout number against "c_1". This has been done in Figure 15 for three organic liquids and water. The calculations are tabulated in Table II in Appendix A.

For prediction purposes this curve is not useful, since $(T_w - T_s)$ at burnout is generally unknown. Therefore a simplified dimensional plot of

$$\frac{(q/A)max}{h_{fg}\rho_v} \text{ vs } \frac{\rho_l - \rho_v}{\rho_v}$$

is presented in Figure 16. The range of variables is greater as there is no limit imposed by the range of the computer results. The quantity $(\rho_l - \rho_v)/\rho_v$ is primarily a function of pressure.

III PHOTOGRAPHIC OBSERVATIONS

In order to frame a satisfactory model for the bubble growth calculations and to examine the cause of departure, it was necessary to get some unconfused motion pictures of bubbles growing. It was decided a side view of a single bubble growing and departing from a vertical surface was best.

For this purpose a small scale atmospheric pressure tank with two lucite sides was built which had a 1/4" diameter heater surface at one end made of copper 3 mils thick. A heater was pressed against this with a pressure just sufficient to cause a single bubble to form. The pictures taken on this apparatus are presented in Figure 17. No attempt was made to measure surface temperature as the localized heating of the surface made such measurements both impractical and meaningless. Several facts of importance can be obtained from these photographs.

In the earliest stages of growth the bubble shape is closely approximated by a hemisphere with the edge tucked under. It can be seen that except for the amount tucked under, this picture would be essentially unchanged for the entire range of bubble sizes from 0° to 90°. The shape of the bubble would be basically hemispherical with only the amount tucked under changing. It is also apparent that the major part of the bubble's growth takes place while the bubble is still in this approximately hemispherical shape. At the time the bubble departs its growth rate has apparently decreased to a very low value. The cause for departure is not immediately apparent from the photographs, as the surface from which the bubble departs is vertical. What is the mechanism causing departure?

It cannot be said that there is a satisfactory answer to this problem at this time. However, several possibilities have been eliminated and one promising one remains. Gravity effects are not significant because the strip is vertical. Another possibility is that when the bubble which is "compressed" into a hemisphere on the surface is released, it tends to rebound into an elongated elipsoid under the influence of surface tension. A check of this possibility indicated that the time of rebound for bubbles of these sizes is too great by a factor of four. If there is a streaming velocity past a bubble on a surface, the possibility exists that aerodynamic lift can draw the bubble off. In this case, however, there is only a very slight natural convection velocity and the departure velocity is far too high to be accounted for by it. The most promising explanation seems to be that the bubble is drawn off the surface by the inertia of the surrounding liquid. The following is a more detailed description of this process.

In the early stages of bubble growth, the growth rate is very large as the liquid superheat is high in the vicinity of the wall and the thickness of the layer

of cooled liquid surrounding the bubble is very small. Therefore, the liquid in front of the bubble has a high forward velocity. As the bubble penetrates into the cooler liquid away from the surface, its growth rate decreases and the rapidly moving liquid in front of the bubble must be decelerated. This creates a low pressure area in front of the bubble which tends to elongate it, and under the proper circumstances, to draw it off the surface. Whether this mechanism can be effective in drawing the bubble off the surface depends in part on the contact angle. From Figure 10 there seems to be a limit in the contact angle with which it is possible to have a clean departure. Such a limit should exist for the following reason.

A 90° contact angle bubble in the absence of gravity would always remain a hemisphere on a plane surface no matter what its growth rate. This is because a spherical bubble in an infinite field of liquid always remains spherical from symmetry considerations, and working with a hemisphere does not alter this symmetry. There is no way then, that the inertia of the liquid surrounding a perfect hemispherical bubble can act to draw it off the surface. However, somewhere between 90° and 0° there is a limiting contact angle below which a bubble can depart cleanly from the surface due to liquid inertia. The photographs indicate that this limit is around 40°. A good mathematical explanation of this departure phenomenon would be welcome. At contact angles greater than this limit but less than 90°, it seems that the bubble can be much elongated by the liquid inertia but the "departure" is a result of an instability of the surface which pinches off the bubble some distance from the heater. When this happens there is a smaller bubble left on the surface which starts to grow immediately. If the boiling is from a horizontal heater surface it can be expected that gravity will aid in drawing the bubble off the surface and the limit of around 40° observed for bubbles departing from a vertical surface would be raised.

These are the important experimental observations: first, in the most rapid stages of growth the shape of a bubble can be approximated by a hemisphere; second, a bubble with a sufficiently small contact angle can depart from a surface independently of the effects of gravity when its growth rate becomes small enough.

CONCLUSIONS

1. For increasing pressure and decreasing c_1 the growth velocity decreases.

2. The maximum size attained by bubbles for small c_1 is independent of "c_1" and depends only on the thickness of the layer of superheated liquid near the surface. (Compare Figures 5 and 6)

3. The average growth velocity of bubbles with a small maximum size is greater than those with a larger maximum size for the same value of c_1.

4. The increased heat flux for a given ΔT obtained with increasing subcooling is in part accounted for by the increased average growth velocity of bubbles with smaller maximum size, (Conclusion 3). This increased average growth velocity causes a more powerful stirring action.

5. Pool boiling burnout data can be correlated using these bubble growth curves.

6. Bubbles can depart from a heater surface as a result of causes other than gravity.

7. This departure occurs when the growth velocity has decreased to a very low value.

8. In the early stages of growth the bubble's shape can be approximated by a hemisphere.

APPENDIX A

Table II

Fluid	P	μ_l	ρ_l	ρ_v	k_l	c_l	$(q/A)_{max} \times 10^{-3}$	$T_w - T_s$
	psia	$lb_m/hr.ft.$	lb_m/ft^3	lb_m/ft^3	$\frac{BTU}{hr.ft.^\circ F}$	$\frac{BTU}{lb_m\,^\circ F}$	$\frac{BTU}{hr.ft^2}$	$^\circ F$
Ethanol	115	.436	41.3	.730	.079	1.009	270	37
	265	.284	37.7	1.785	.072	1.175	330	33
	515	.190	33.3	4.01	.065	1.387	330	24
	765	.153	27.2	7.85	.055	1.532	170	9
Benzene	115	.360	44.5	1.186	.069	.556	216	46
	265	.237	41.0	2.87	.060	.606	240	29
	465	.151	34.1	6.18	.054	.647	200	14
n-Pentane	60	.354	34.8	.705	.073	.596	140	46
	115	.284	32.4	1.34	.071	.614	165	37
	215	.215	29.0	2.78	.068	.648	170	26
	315	.177	25.9	4.49	.066	.666	123	18
	415	.142	22.6	7.13	.060	.680	72	8
Water	383	.294	52.0	.818	.368	1.12	1,350	60
	770	.249	48.4	1.69	.340	1.22	1,600	55
	1205	.222	44.9	2.88	.316	1.37	1,550	38
	1602	.207	41.9	3.94	.287	1.59	1,450	35
	1985	.192	39.0	5.29	.262	1.80	1,280	25
	2460	.172	35.4	7.46	.220	3.20	900	14

Table II cont.

Fluid	P	c_l	v	Y	$b \times 10^5$	$D_B \times 10^4$	$t \times 10^7$	fD_b	$\frac{(q/A)max}{h_{fg} \rho_v f(D_b)}$
	psia	--	-	-	ft	ft	hr	ft/hr	-
Ethanol	115	7.06	4	3.9	4.49	2.78	2.65	524	2.37
	265	3.25	2.5	2.32	4.75	1.76	3.47	254	2.89
	515	1.49	2.27	1.49	5.49	1.3	5.33	122	3.63
	765	.475	1.6	.80	7.67	9.75	7.73	63	3.45
Benzene	115	6.9	3.80	3.8	5.05	3.06	2.39	640	2.05
	265	2.18	2.37	1.89	6.44	1.93	4.25	227	3.17
	465	.595	1.75	.90	7.85	1.12	6.23	90	4.28
n-Pentane	60	10.5	8.1	5.6	5.48	4.86	2.13	1140	1.35
	115	4.76	2.80	2.95	5.71	2.69	2.29	588	1.84
	215	1.94	2.35	1.75	7.36	2.04	3.76	271	2.45
	315	.935	2.05	1.15	9.40	1.73	3.83	141	2.62
	415	.374	1.35	.65	12.6	1.30	10.2	63.9	3.46
Water	383	5.6	3.0	3.3	5.49	2.88	1.21	1190	1.765
	770	2.74	2.54	2.15	6.35	2.17	1.735	625	2.18
	1205	1.38	2.25	1.45	7.88	1.82	3.06	297	2.97
	1602	1.075	2.10	1.25	8.10	1.61	3.64	222	3.08
	1985	.719	1.9	1.0	8.74	1.39	5.1	137	3.77
	2460	.369	1.35	.65	9.85	1.02	8.3	61.5	5.30

APPENDIX B

BIBLIOGRAPHY

1. Forester, H. K. and N. Zuber, "Dynamics of Vapor Bubbles and Boiling Heat Transfer," Conference on Nuclear Engineering, 1955, Los Angeles, California.
2. Forester, H. K. and N. Zuber, "Growth of a Vapor Bubble in a Superheated Liquid," Journal of Applied Physics, Vol. 25, 1954.
3. Ellion, M., "Study of the Mechanism of Boiling Heat Transfer," JPL Memo 20-S8, March 1954, Pasadena, California.
4. Zwick, S. A., "The Growth and Collapse of Vapor Bubbles," Report No. 21-19, ONR, Contract N6 onr 24420, (NR 062-059), 1954.
5. Dergarabedian, P., "Rate of Growth of Vapor Bubbles in Superheated Water," Journal of Applied Mechanics, Vol. 20, p 537, 1953.
6. Rohsenow, W. M. and J. A. Clark, "A Study of the Mechanism of Boiling Heat Transfer," Transactions of the American Society of Mechanical Engineers, Vol. 73, p 609, 1951.
7. Rohsenow, W. M. and P. Griffith, "Correlation of Maximum Heat Flux Data for Boiling of Saturated Liquids," Presented at the American Institute of Chemical Engineers meeting, Louisville, Kentucky, March 1955.
8. Rohsenow, W. M., "A Method of Correlating Heat Transfer Data for Surface Boiling of Liquids," Transactions of the American Society of Mechanical Engineers, July 1952.
9. Gunther, F. C. and F. Kreith, "Photographic Study of Bubble Formation in Heat Transfer to Subcooled Water," Heat Transfer and Fluid Mechanics Institute, 113, Berkley, 1949
10. Taggart, Arthur F. and Nathaniel Arbiter, "Collector Coatings in Soap Flotation," AIME Trans, 153, 501, 1943.
11. Jakob, M. Heat Transfer, Vol. 1, Chap. 30, Wiley, New York, 1948.

APPENDIX C

NOMENCLATURE

A - Area

C_q - Defined by Equation 15

C_{vb} - Defined by Equation 14

D_b - Bubble diameter

Q - Heat

R - Bubble radius

T - Temperature

V - Velocity

Y - $\frac{R}{b}$ Dimensionless bubble radius

b - Thickness of hot layer of liquid near the surface (Figure 2)

c_1 - $\frac{\rho_\ell c_\ell (T_w - T_s)}{\rho_v h_{fg}}$

c_ℓ - Liquid specific heat

f - Bubble frequency

h_{fg} - Latent heat of vaporization

k_ℓ - Liquid thermal conductivity

n - number of bubbles/unit area

q - Heat flux

r - Radius coordinate

t - Time

v - Dimensionless velocity defined by Equation 12 = $Vb\left(\frac{\rho_\ell c_\ell}{k_\ell}\right)$

w - Mass

y - Dimensionless radius coordinate = r/b

θ - Dimensionless temperature $\frac{T - T_b}{T_w - T_b}$

φ - Angular coordinate in spherical coordinates

τ - Dimensionless time $\frac{k_\ell t}{\rho_\ell c_\ell b^2}$

ρ - Density

Subscripts

b - Bulk

l - Liquid

s - Saturation

v - Vapor

w - Wall

FIGURE CAPTIONS

Figure 1. Original hemisphere of liquid and resulting bubble.

Figure 2. The assumed temperature distribution with the knee of the assumed temperature distribution a distance "b" from the heater surface.

Figure 3. Comparison of measured and calculated rates of growth. Solid curve is from interpolation on Figure 8.

Figures 4, 5, 6. Calculated bubble growth rates in dimensionless form.

Figure 7. Calculated bubble growth rates for saturated bulk temperature $\Theta_s = \Theta_b = 0$.

Figure 8. Calculated bubble growth rates for initially uniformly superheated liquid and a spherical bubble.

Figure 9. Cross plots of Figures 4, 5 and 6 for $\tau = 0.25$ and $\Theta_b = 0$.

Figure 10a. Bubble growing and departing cleanly.

10b. Bubble growing and departing cleanly.

10c. Bubble growing and departing with small bubble being left on surface. This bubble starts to grow immediately.

Conditions for Figure 10:

Fluid	-	Water
Pressure	-	1 atmosphere
T_{bulk}	-	211°F
T_{wall}	-	Unknown
Camera speed	-	2500 frames/sec
Scale	-	2.25 times actual size

Time increases down and to the right and gravity acts to make bubbles rise on picture.

Figure 11. Plot showing burnout point.

Figure 12. Bubbles packed on the surface.

Figure 13. The assumed temperature distribution near the surface.

Figure 14. The effect of c_1 on the thickness of the cooled layer surrounding the bubble.

Figure 15. Dimensionless burnout correlation

Figure 16. Dimensional burnout correlation.

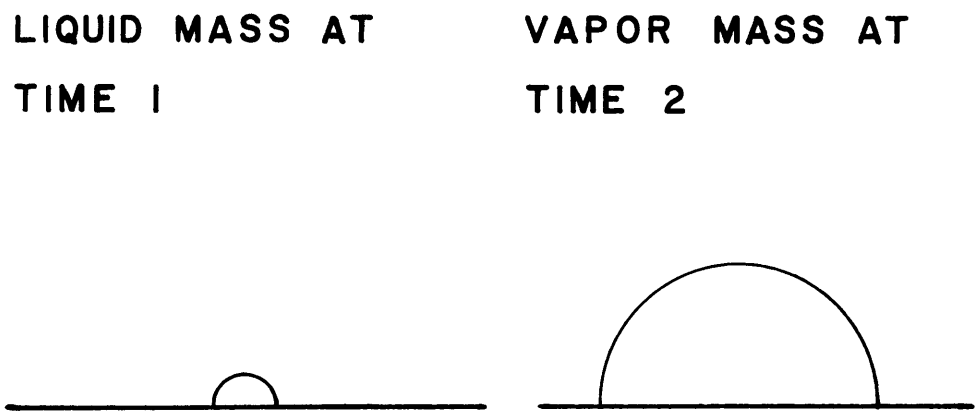

FIGURE 1

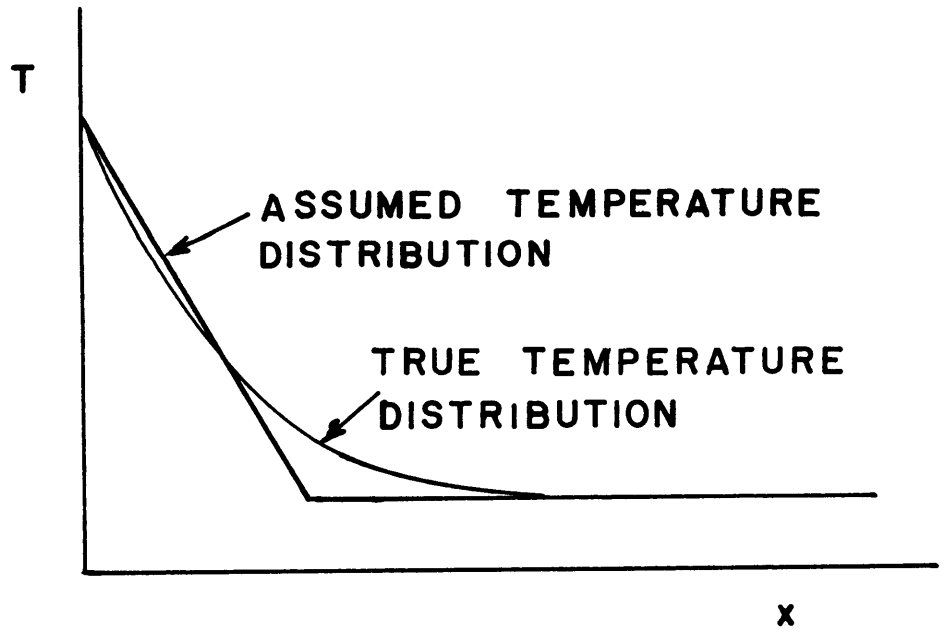

FIGURE 2

FIGURE 3

COMPARISON OF CALCULATED AND MEASURED GROWTH RATES

FLUID - WATER
P = 1 ATMOSPHERE

T = 103.1 ^{0}C

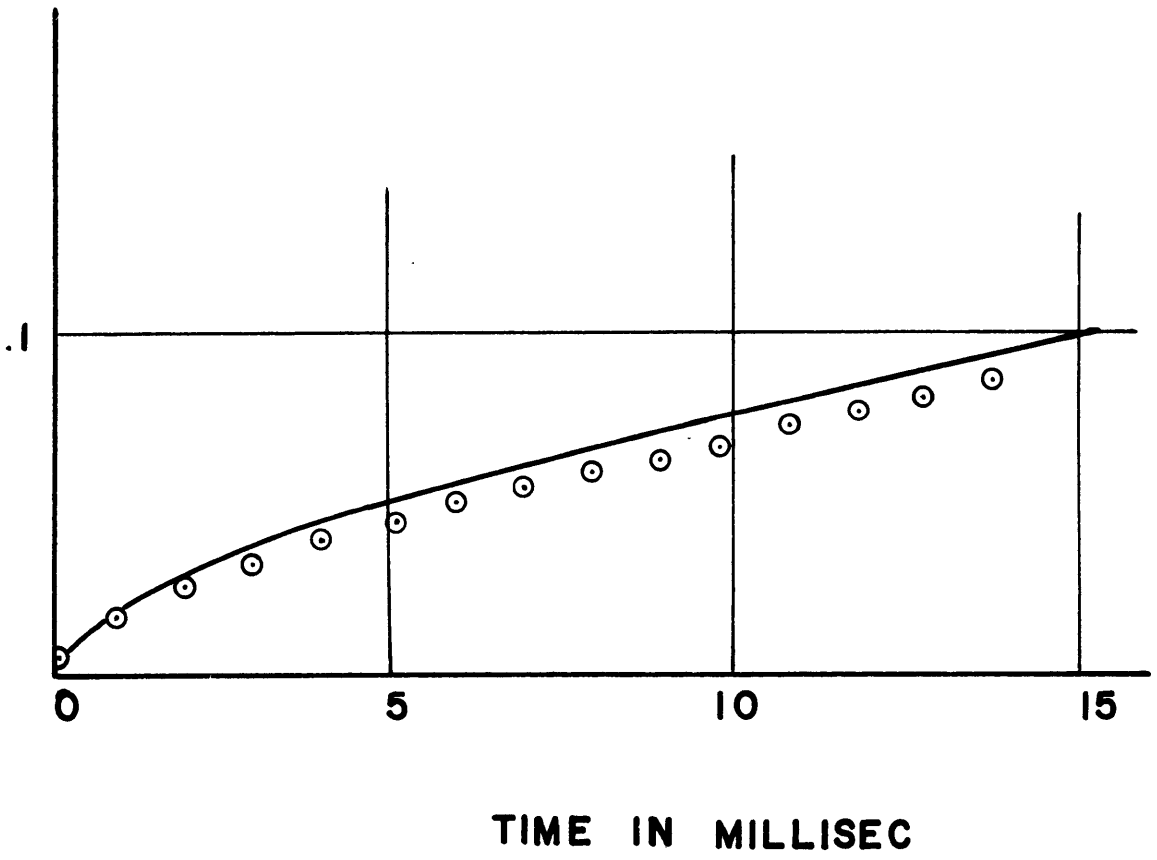

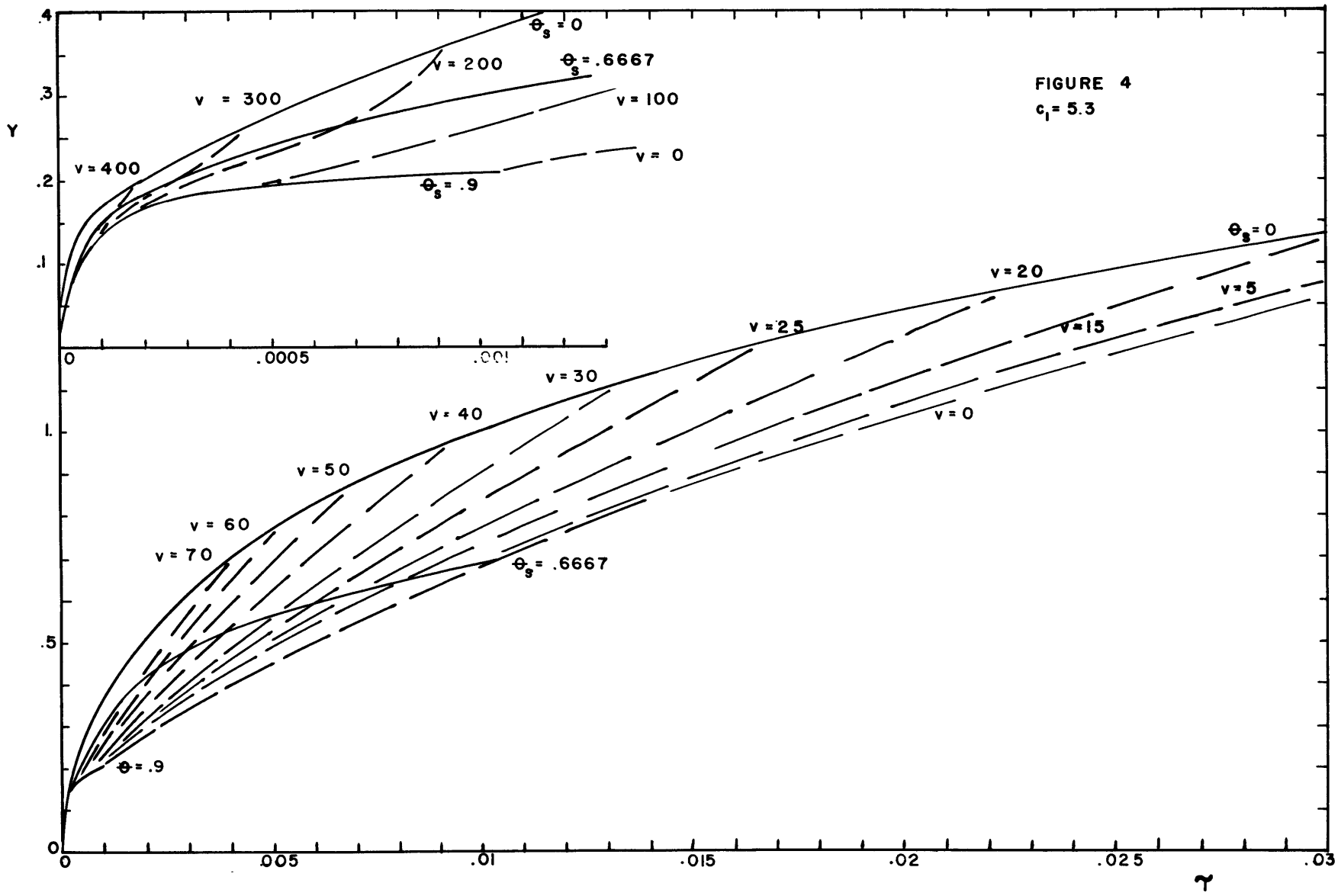
FIGURE 4
$c_1 = 5.3$
Y
τ
$\theta_s = 0$
$\theta_s = .6667$
$\theta_s = .9$
$\theta = .9$
v = 300
v = 200
v = 100
v = 0
v = 400
v = 20
v = 5
v = 25
v = 15
v = 30
v = 40
v = 50
v = 60
v = 70
0
.0005
.001
.005
.01
.015
.02
.025
.03
.1
.2
.3
.4
.5
1.

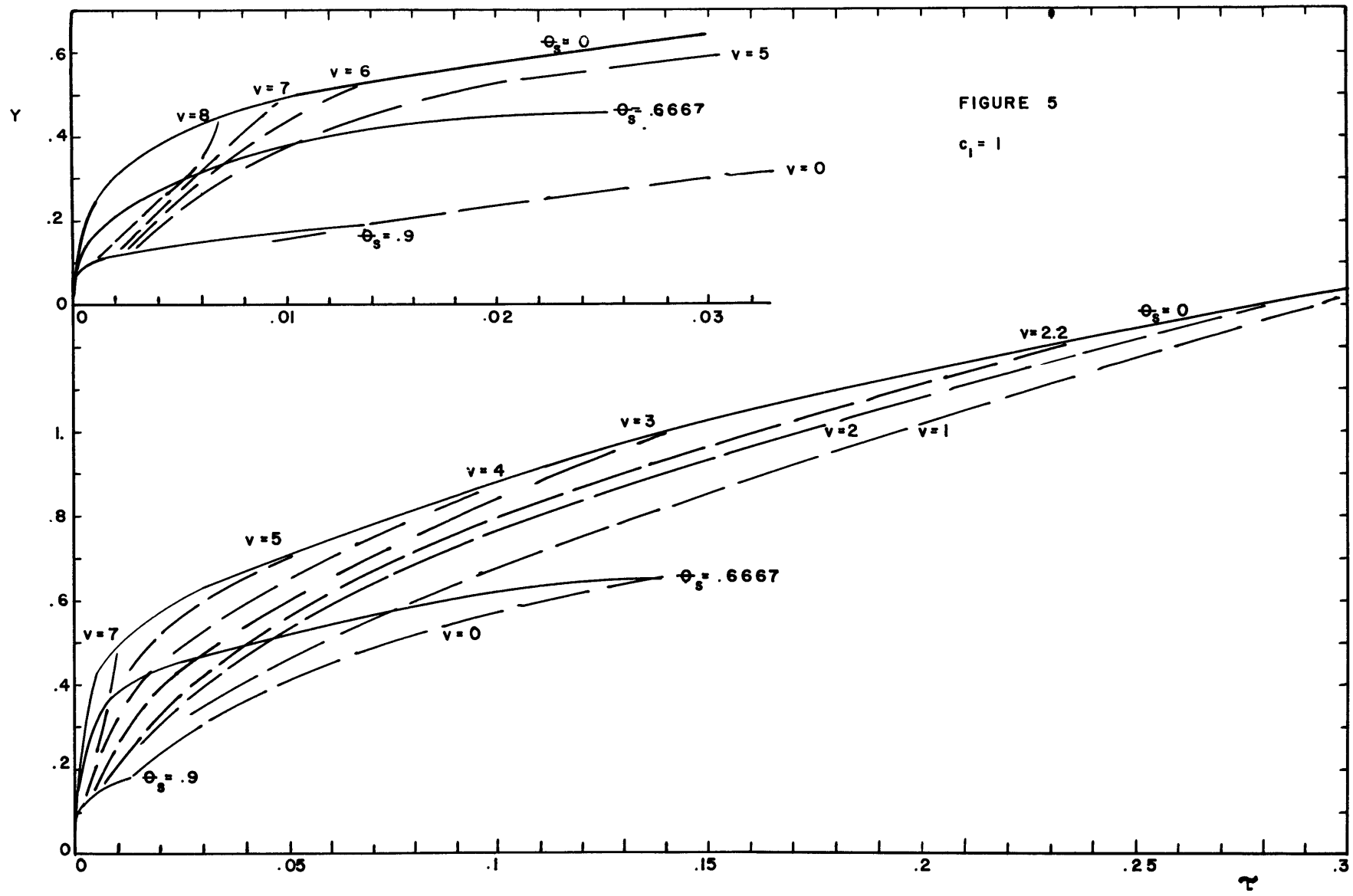
Y
τ
$\Theta_s = 0$
$\Theta_s = .6667$
$\Theta_s = .9$
v = 0
v = 1
v = 2
v = 2.2
v = 3
v = 4
v = 5
v = 6
v = 7
v = 8
0
.01
.02
.03
.05
.1
.15
.2
.25
.3
.2
.4
.6
.8
1.

FIGURE 5

$c_1 = 1$

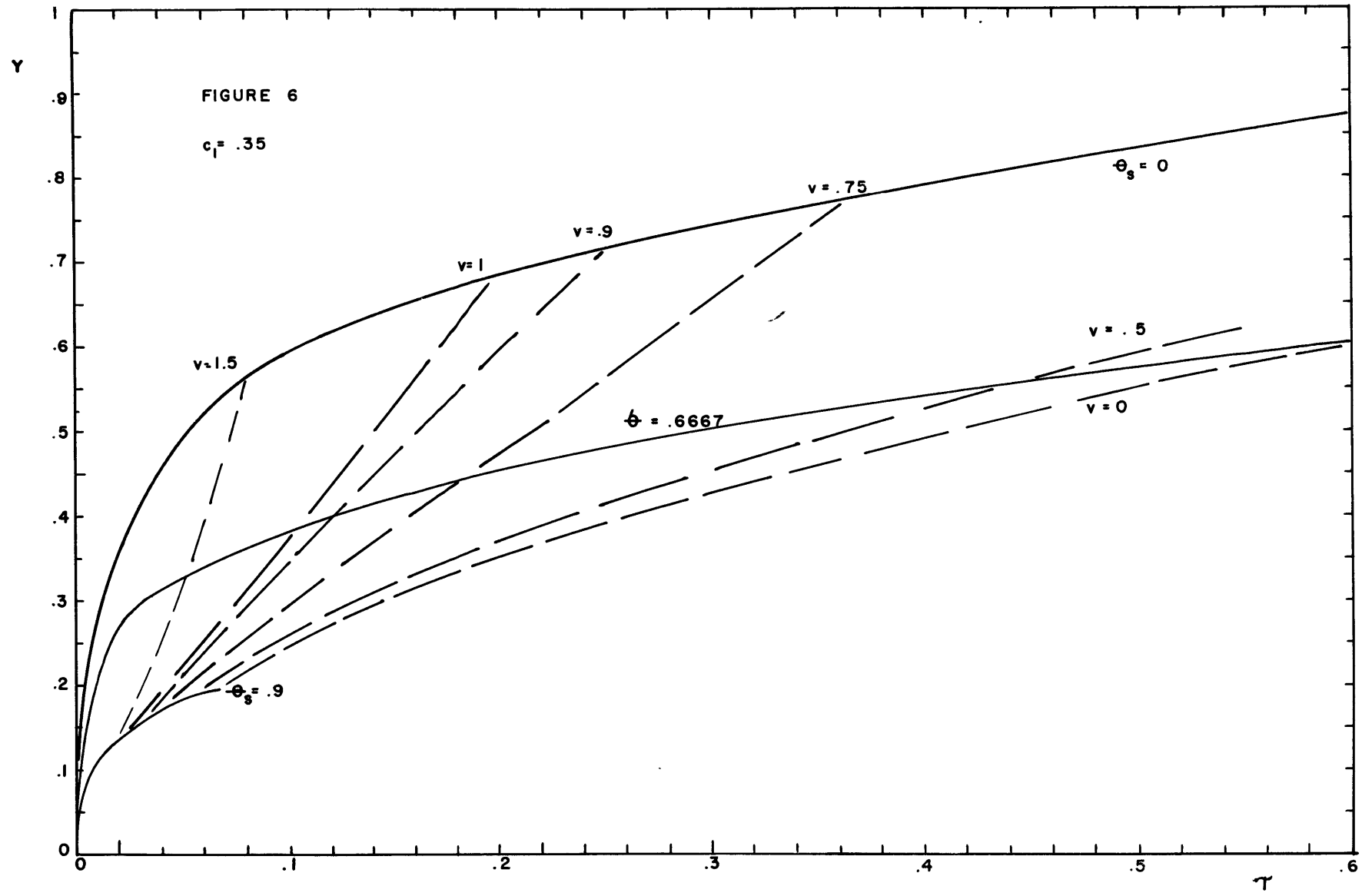
FIGURE 6
c_1 = .35
Y
T
θ_s = 0
v = .75
v = .9
v = 1
v = 1.5
v = .5
v = 0
θ = .6667
θ_s = .9
0
.1
.2
.3
.4
.5
.6
.7
.8
.9
1

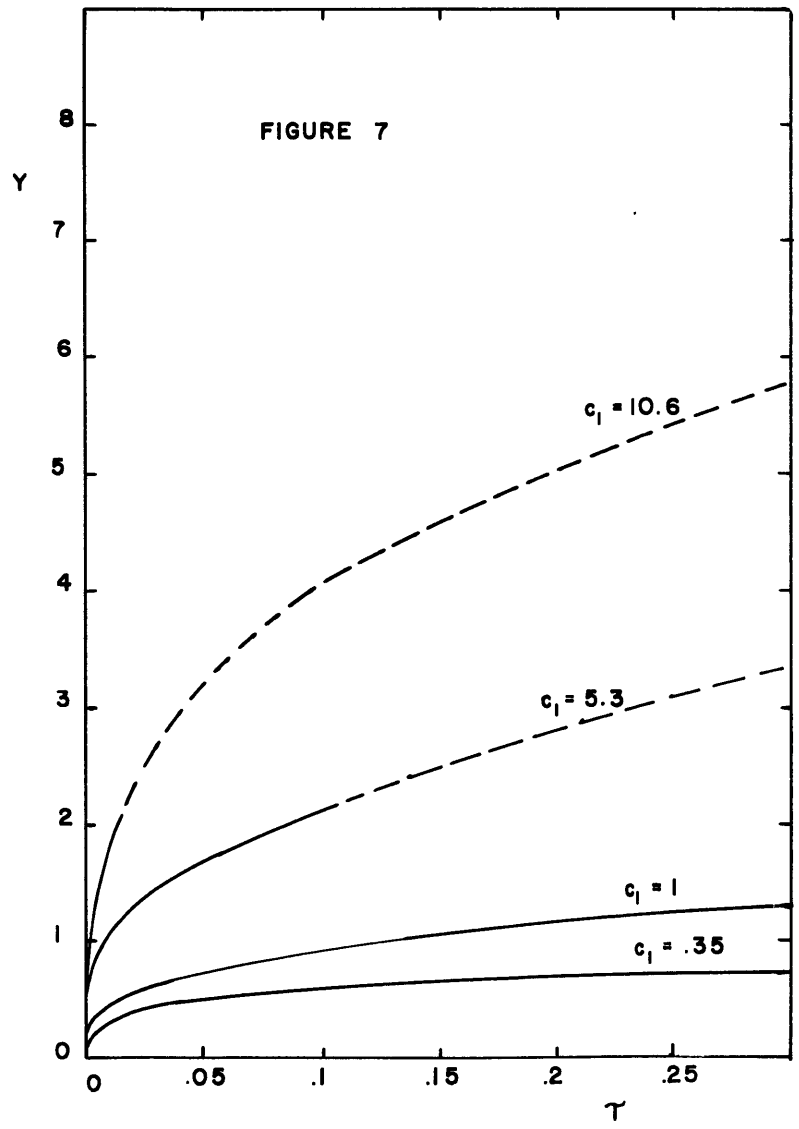
FIGURE 7
Y
8
7
6
5
4
3
2
1
0
c_1 = 10.6
c_1 = 5.3
c_1 = 1
c_1 = .35
0
.05
.1
.15
.2
.25
τ

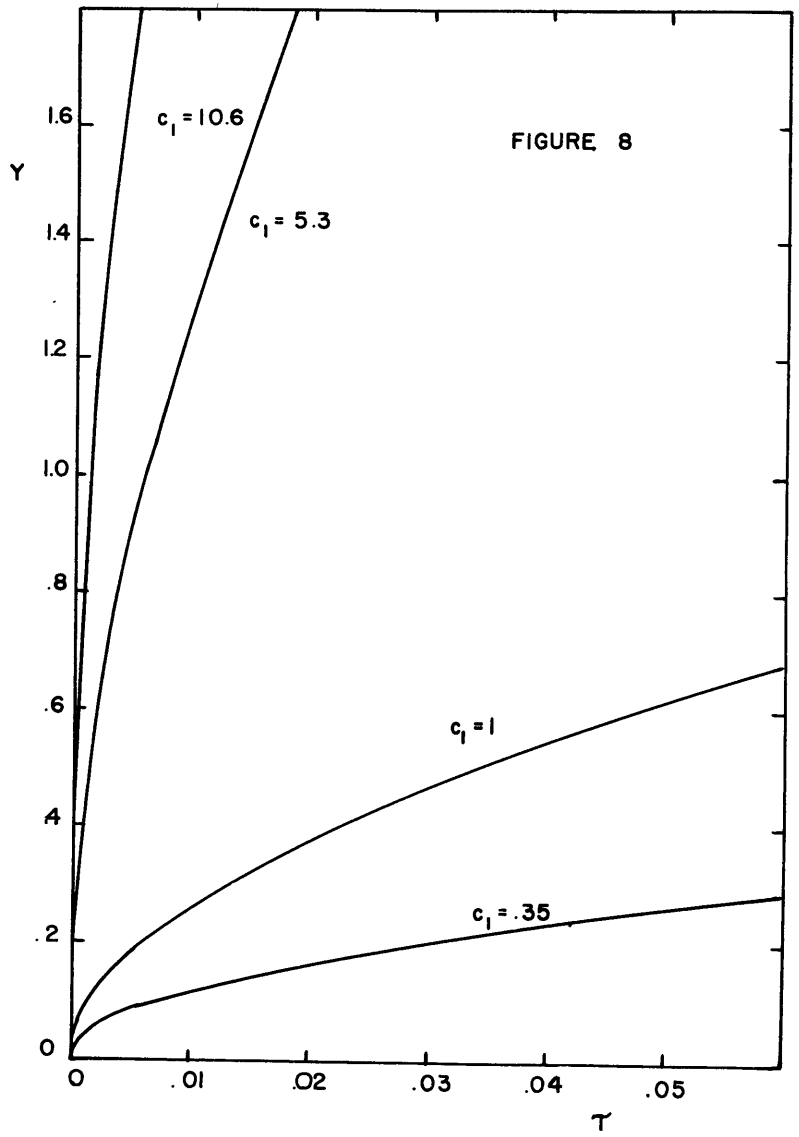
FIGURE 8
Y
1.6
1.4
1.2
1.0
.8
.6
4
.2
0
c_1 = 10.6
c_1 = 5.3
c_1 = 1
c_1 = .35
0
.01
.02
.03
.04
.05
τ

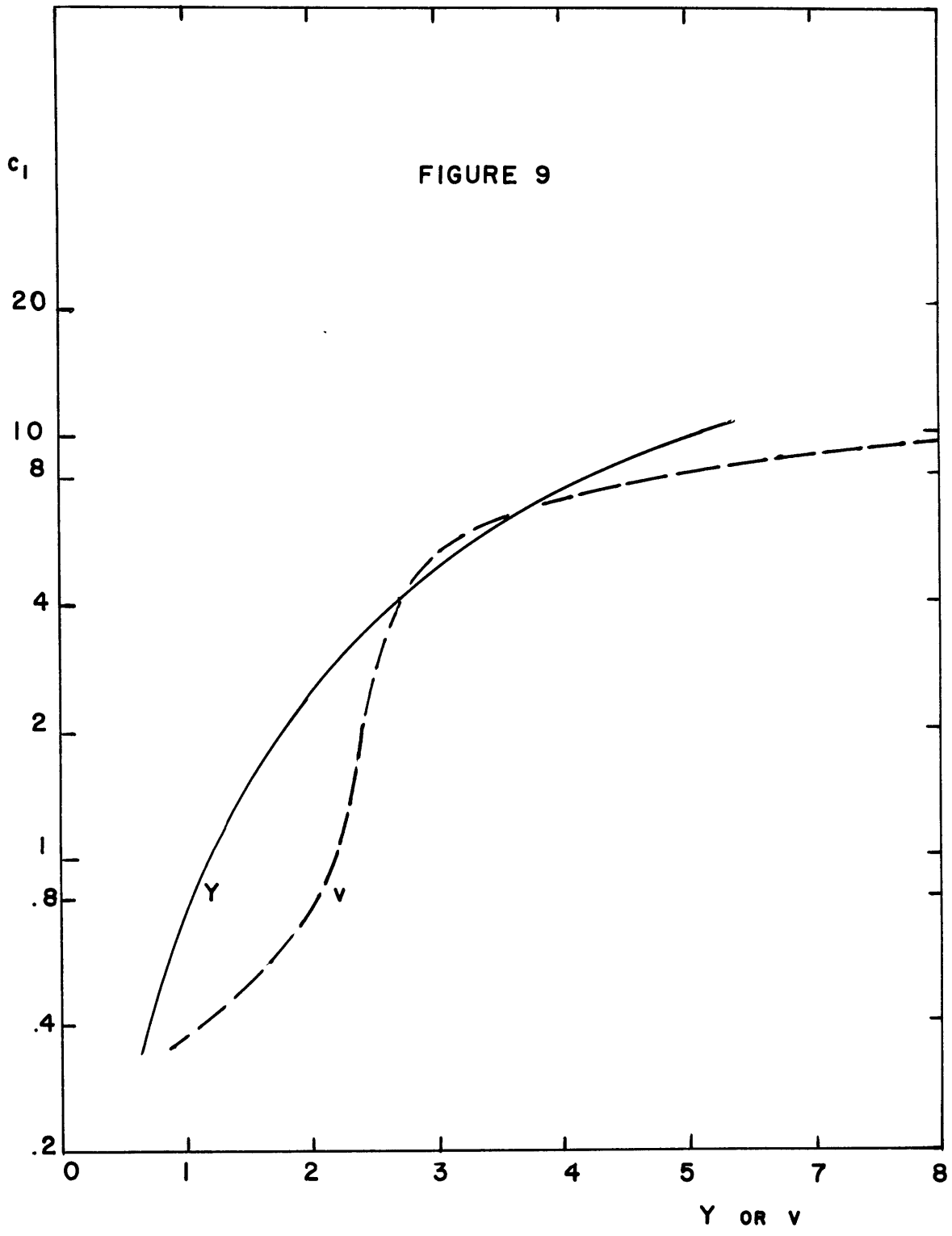
FIGURE 9
c_1
20
10
8
4
2
1
.8
.4
.2
0
1
2
3
4
5
7
8
Y
v
Y OR v

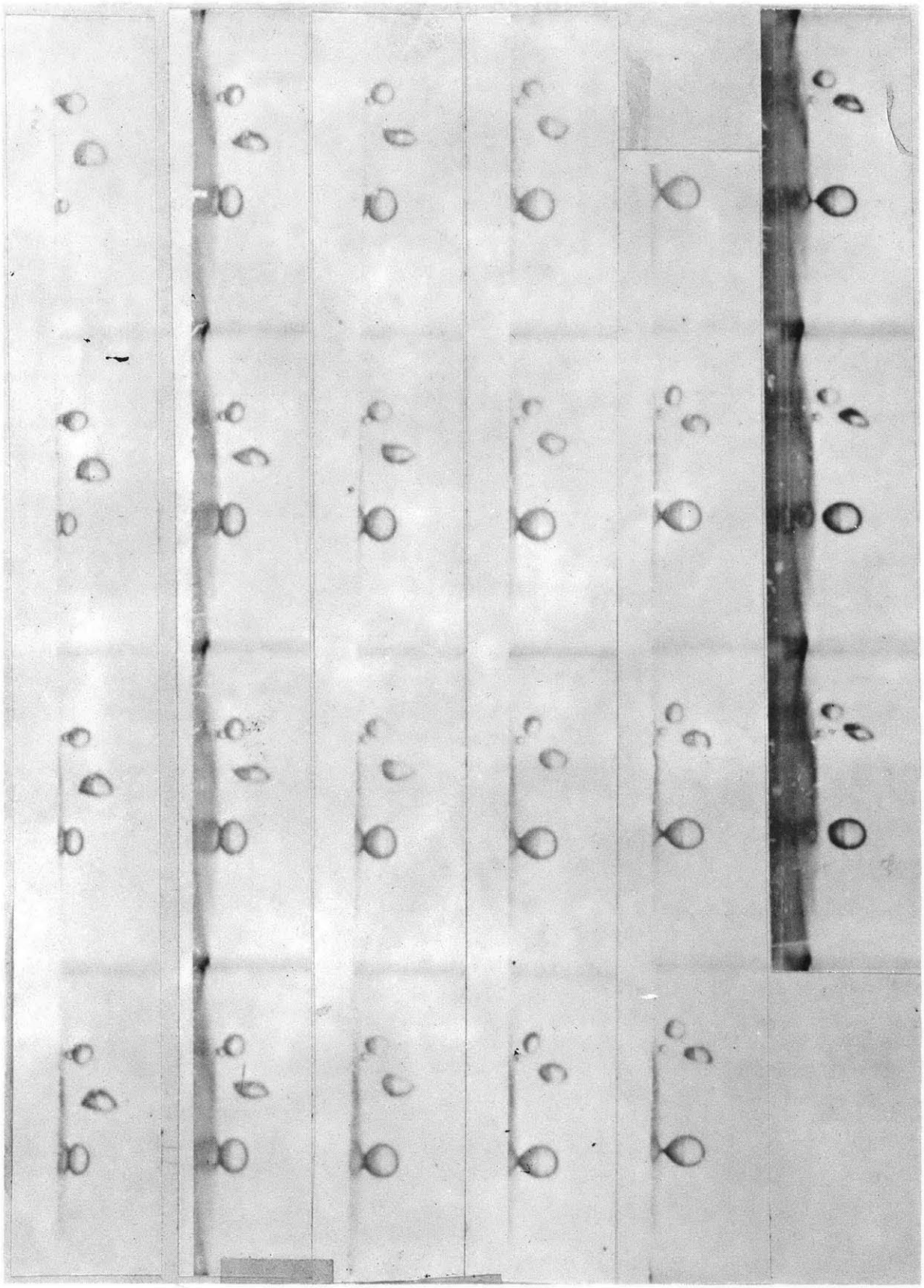

FIGURE 10A

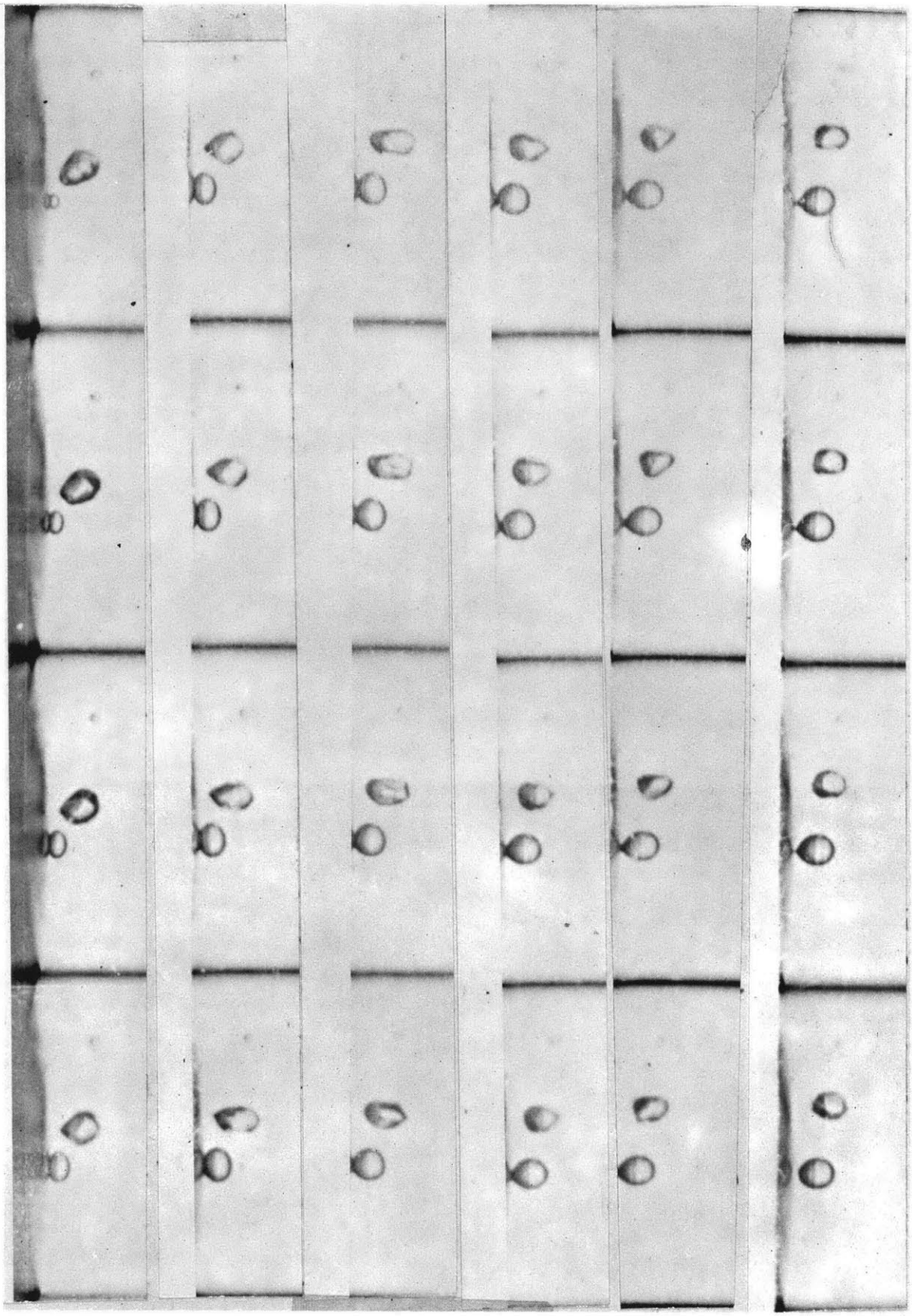

FIGURE 10B

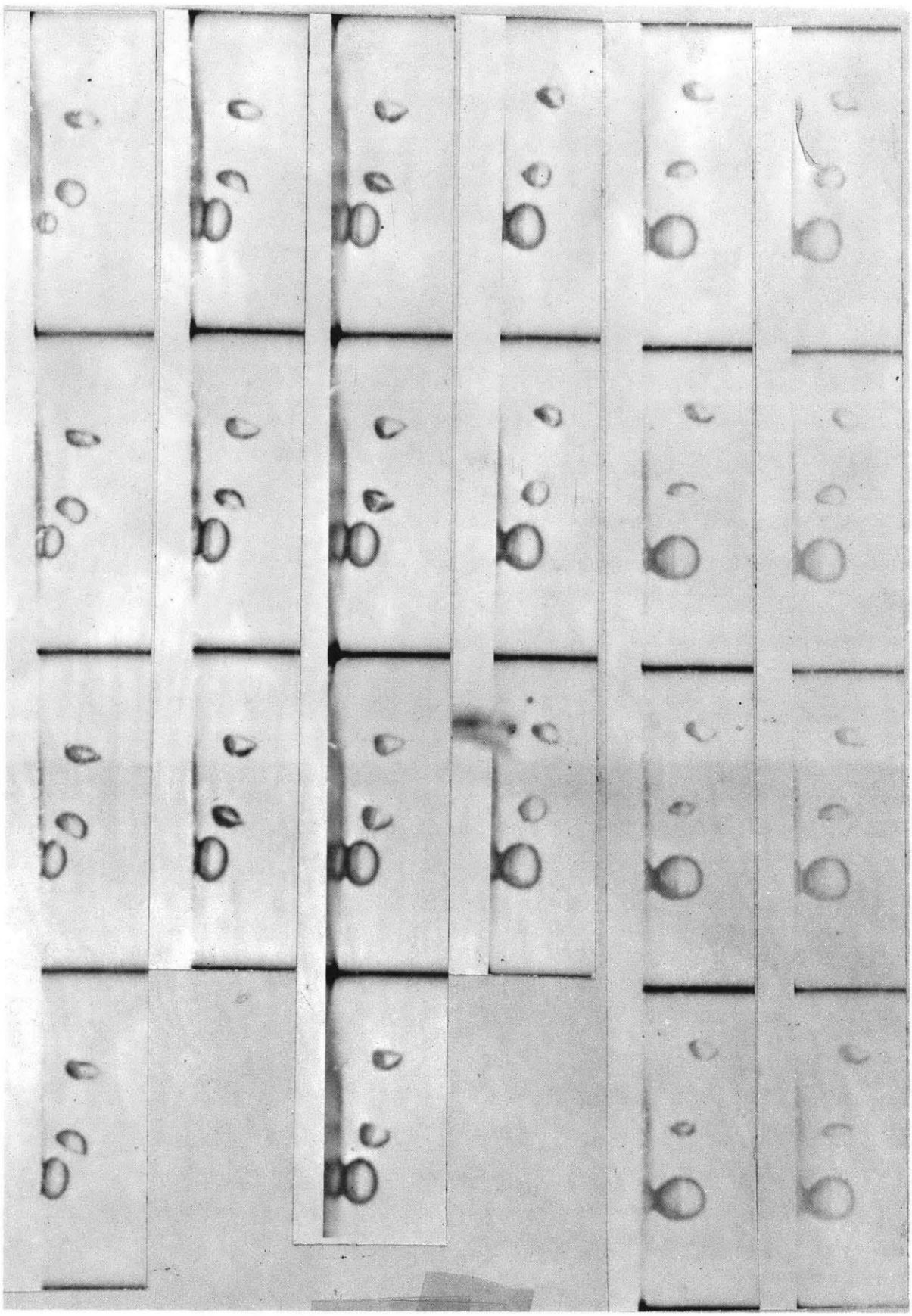

FIGURE 10C

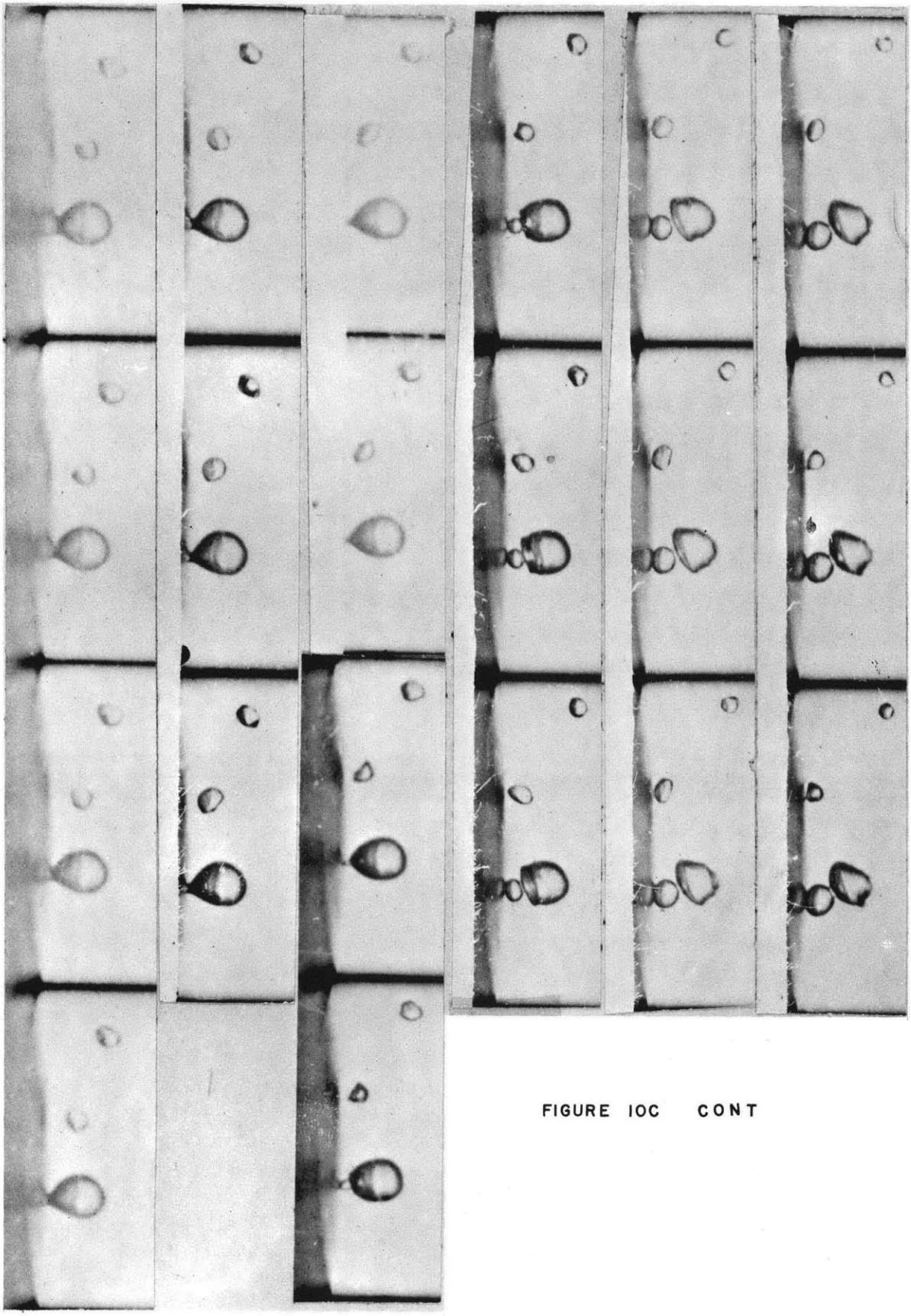

FIGURE 10C CONT

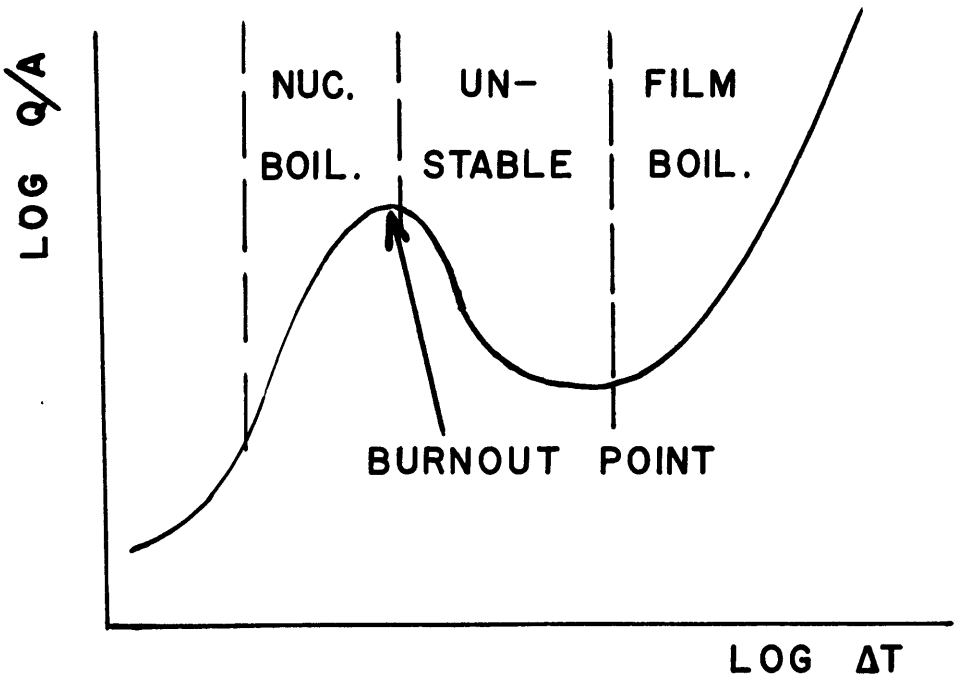

FIGURE 11

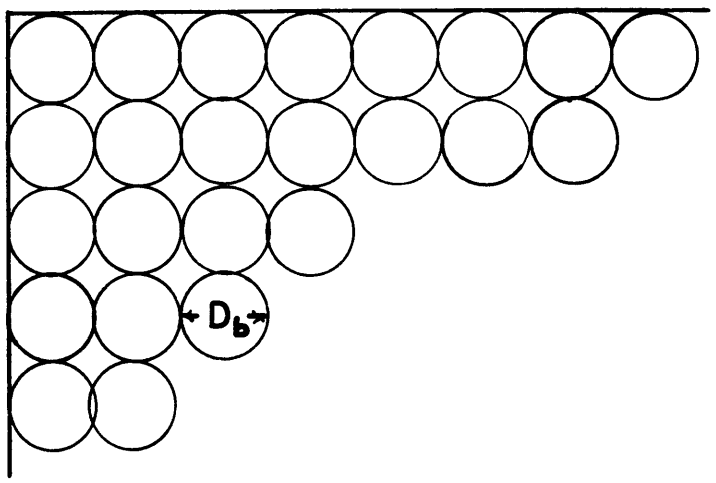

FIGURE 12

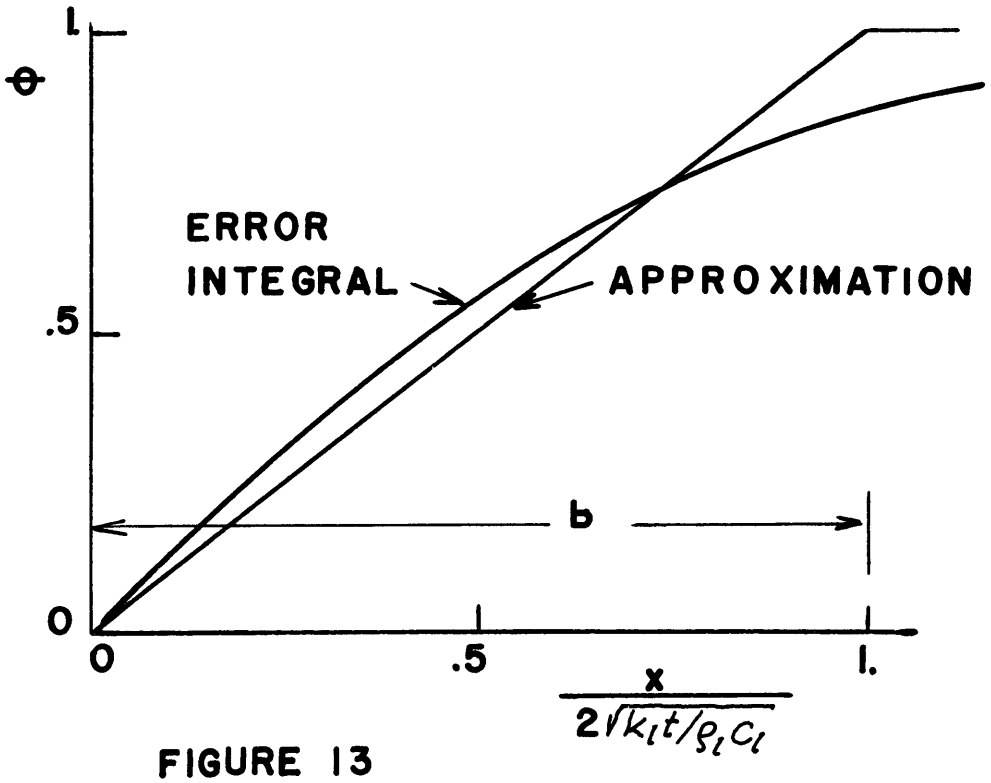

FIGURE 13

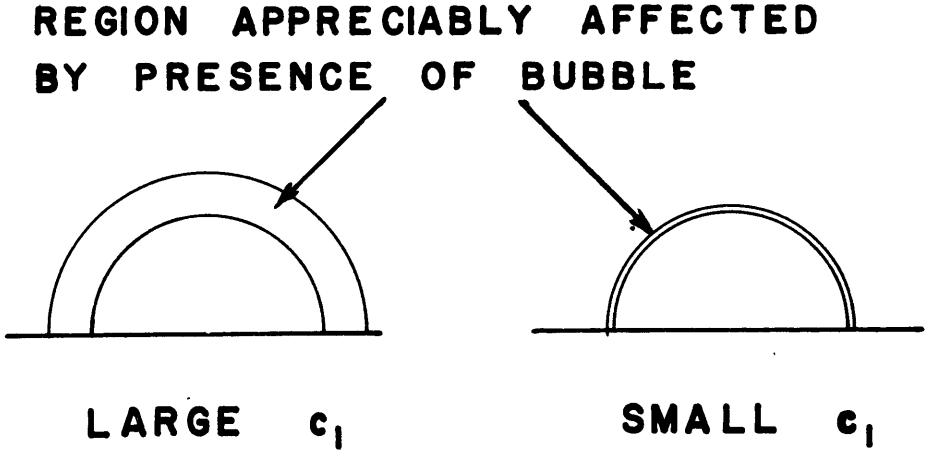

FIGURE 14

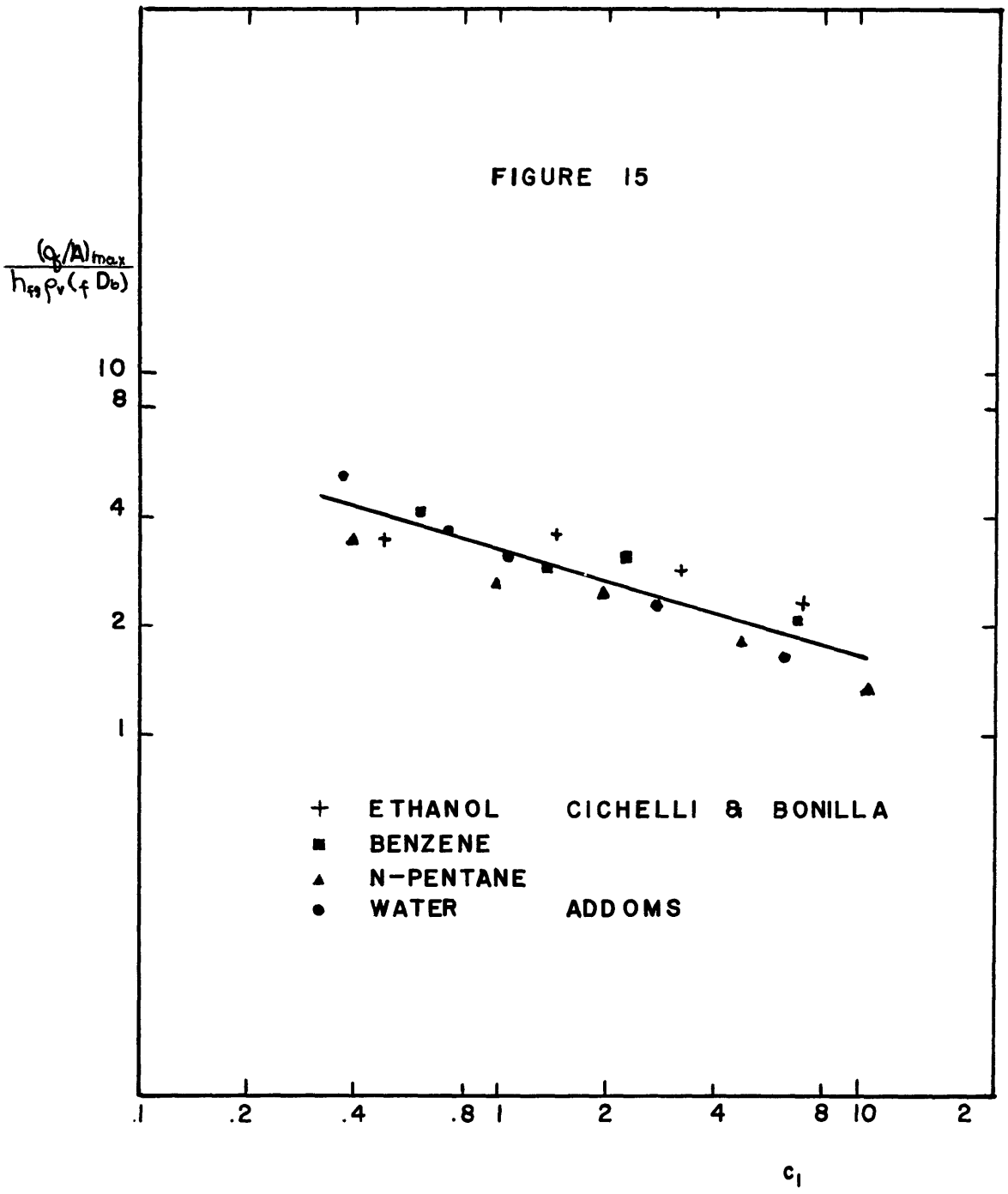
FIGURE 15
$\frac{(q_f/A)_{max}}{h_{fg}\rho_v(f D_b)}$
10
8
4
2
1
.1
.2
.4
.8
1
2
4
8
10
2
c_1
+ ETHANOL
■ BENZENE
▲ N-PENTANE
● WATER
CICHELLI & BONILLA
ADDOMS

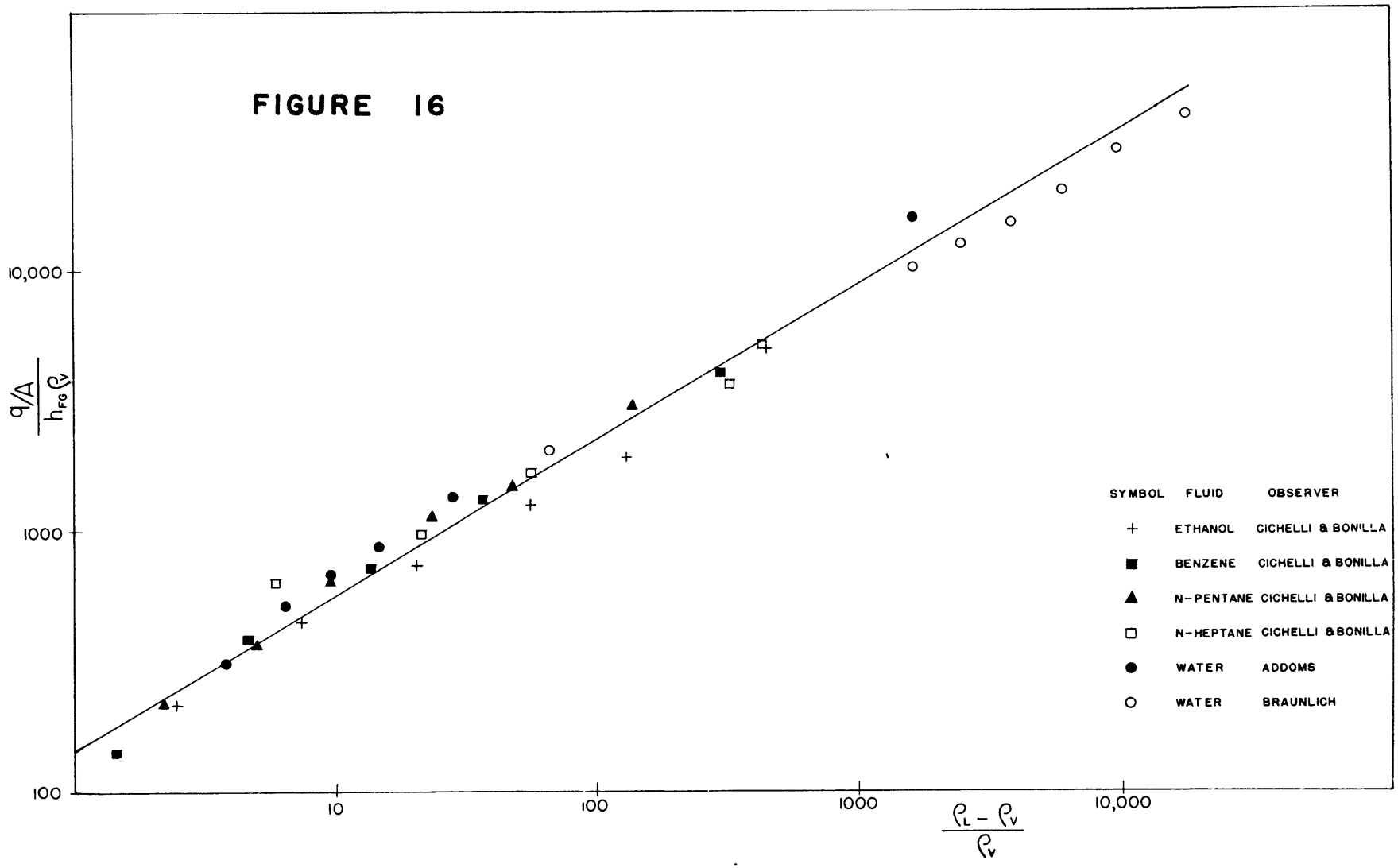
FIGURE 16
10,000
1000
100
10
100
1000
10,000
$\frac{q/A}{h_{FG}\rho_v}$
$\frac{\rho_L - \rho_v}{\rho_v}$
SYMBOL FLUID OBSERVER
+ ETHANOL CICHELLI & BONILLA
■ BENZENE CICHELLI & BONILLA
▲ N-PENTANE CICHELLI & BONILLA
□ N-HEPTANE CICHELLI & BONILLA
● WATER ADDOMS
○ WATER BRAUNLICH